

ON PHYSICAL AND DATA DRIVEN MODELLING OF IRRIGATION CHANNELS

Su Ki Ooi¹ M.P.M. Krutzen² E. Weyer¹

¹*CSSIP, Department of Electrical and Electronic Engineering, The
University of Melbourne, Parkville, VIC 3010, Australia.*

Email: {skoo, e.weyer}@ee.mu.oz.au

²*DMP - Control Engineering Group, TNO Institute of Applied Physics,
P.O. Box 155, 2600 AD DELFT, The Netherlands.*

Email: krutzen@tpd.tno.nl

Abstract: In this paper we compare the St. Venant equations against real data in order to examine their accuracy and capability to describe the relevant dynamics of an irrigation channel. The St. Venant equations are simulated using the Preissmann scheme, and the simulated and real measured water levels are compared. In addition, a comparison with system identification models is also performed in order to examine which model is more suitable for control design and prediction purposes. The results show that the St. Venant equations can adequately capture the dynamics of the real channels. However, system identification methods are as accurate as the St. Venant equations and are preferred over the St. Venant models for control and prediction purposes since they are much simpler to use.

Keywords: Modelling, system identification, physical modelling, parameter estimation, environmental systems, irrigation channel.

1. INTRODUCTION

Due to the sharp rise in demand for water in many parts of the world, water is becoming an increasingly scarce resource. It is therefore important to manage the water resources well and minimize the losses. This applies particularly to networks of irrigation channels, where large amounts of water are wasted due to poor management and control. These losses can be reduced by improving the decision support and control systems in the channels.

In order to design a good controller or a decision support system, most design methods require a good model that closely describes the relevant dynamics of the irrigation channel. Traditionally, the dynamics are modelled by the St. Venant equations, see e.g. (Chaudhry, 1993). The St.

Venant equations are commonly used for prediction and control design for irrigation channels, see (Malaterre and Baume, 1998) for an overview. Despite widespread use, their accuracy are largely unknown which is surprising, taking into account the large amount of practically oriented research which uses the St. Venant equations as a starting point. A natural question is therefore whether the St. Venant equations are capable of describing the relevant dynamics of an irrigation channel accurately? From laboratory experiments (Brutsaert, 1971), it is known that the St. Venant equations are an accurate representation of a small scale laboratory channel. To the authors' knowledge, very few, if any of the models based on the St. Venant equations have been tested against data from real channels, which can be several kilometers long and the channel geometry is often nonuniform. In this paper,

comparison of the St. Venant equations against real data is considered in order to examine their accuracy.

Previous works (see e.g. (Weyer, 2001) and (Ooi and Weyer, 2001)) showed that simple models that describe the dynamics of the channel adequately can be obtained using system identification method based on operational data from the channel. The St. Venant equations are hyperbolic partial differential equations and much more complex to use than the system identification models, and an open question is whether the St. Venant equations are significantly more accurate than the system identification models. We therefore also compare the performance of the models based on the St. Venant equations and the system identification models. In particular we examine their suitability for control design and prediction purposes.

The best known and most used finite difference method for solving the St. Venant equations is the Preissmann scheme (see e.g. (Chaudhry, 1993)). In order to examine the accuracy of the St. Venant equations, the water level in the channel is simulated using the Preissmann scheme based on physical data from the channel, such as length, width, etc, and the simulated water level is compared against the measured water level. There are parameters in the St. Venant equations which are not exactly known. In order to examine the effect of those parameters on the accuracy of the St. Venant equations, these parameters are estimated from the observed data, and the accuracy of the St. Venant equations with estimated and physical parameters is examined. This is followed by a comparison with system identification models, comparing the simulated water levels of the respective models with the measured water level.

In Section 2 a description of the irrigation channel is given. Then, the St. Venant equations are presented and the Preissmann scheme is briefly explained. The accuracy of the St. Venant equations is investigated in Section 4, followed by a comparison with system identification models. Finally, conclusions are given in Section 6.

2. CHANNEL DESCRIPTION

The channel considered in this paper is the Houghton Main Channel (HMC) in Queensland, Australia. Figure 1 shows a schematic side view of the channel. The channel is automated with overshoot gates as shown in Figure 1. We refer to the stretch of the channel between two gates as a pool. We name the pool according to the number of the upstream gate, e.g. the pool in Figure 1 is pool i . y_i and y_j are the upstream water level of gate i and j respectively, and p_i and p_j are the position of gates. The amount of water above the gate is called the head over the gate, and denoted by h_i and h_j .

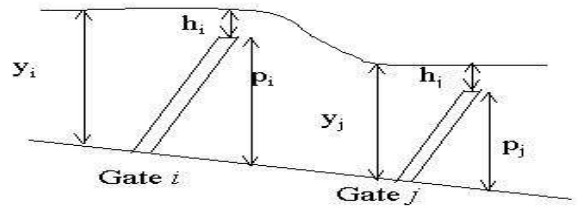


Fig. 1. Schematic of channel with overshoot gates

The water levels, given in mAHD (meter Australia Height Datum), and the gate positions are the measured variables. The head over gate is computed from these variables. A fully shut gate has position of 0 meter and a positive value when the gate is open. The measured gate position, $\bar{p} = p_{max} - p$, where p_{max} is the position when the gate is fully shut. The head over the gate i and j is calculated as $h_i = y_i + \bar{p}_i - a_i$ and $h_j = y_j + \bar{p}_j - a_j$, where a_i and a_j are the gate adjustment constants necessary to convert from mAHD to meter.

3. ST. VENANT EQUATIONS

The St. Venant equations are derived from a mass and momentum balance, see e.g. (Chaudhry, 1993) and given by

$$\begin{aligned} \frac{\partial A}{\partial t} + \frac{\partial Q}{\partial x} &= 0 \\ \frac{\partial Q}{\partial t} + \left(\frac{gA}{B} - \frac{Q^2}{A^2} \right) \frac{\partial A}{\partial x} + \frac{2Q}{A} \frac{\partial Q}{\partial x} + gA(S_f - \bar{S}) &= 0 \end{aligned} \quad (1)$$

where A is the cross sectional area of the channel, B is the width of the water surface, $g = 9.81m/s^2$ is the gravity, \bar{S} is the bottom slope, Q is the flow (discharge), and S_f is the friction slope. A commonly used relationship between the flow and the head over gate is $Q = ch^{3/2}$ (see e.g. (Chaudhry, 1993)), where c is the gate constant. The gate constant of the upstream and downstream gate are labelled as c_{in} and c_{out} . From (Fenton, 2001), for a sharp-edged rectangular weir, $c \approx 0.6\sqrt{gb}$ where b is the gate width.

According to the Manning equation, $S_f = \frac{n^2 Q^2}{A^2 R^{4/3}}$ where n is the Manning coefficient, which mainly depends on the surface roughness. Table values of n for different flow surfaces are available (see e.g. <http://www.lmnoeng.com/manningn.htm>). $R = \frac{A}{P}$ is the hydraulic radius, where the wetted perimeter, P , is defined as the length of line of intersection of the channel's wetted surface with a cross-sectional plane normal to the flow (see (Chaudhry, 1993)).

The pools we study are pool 9 and 10 of the HMC. The physical data are given in Table 1. The Manning coefficients are taken from www.lmnoeng.com/manningn.htm

for clean excavated earth channels. Obviously, the physical data listed in Table 1 are approximate values since the real condition of the channel will change with time and along the channel, and some parameters like the gate constant cannot be accurately measured or computed.

	Pool 9	Pool 10
Length, L	853m	3129m
Bottom width	6m	6m
Side slope	2	2
Bottom slope	1.993×10^{-4}	9.907×10^{-5}
Gravity, g	9.81 m/s^2	9.81 m/s^2
Gate width, b	4.4m	4.4m
Manning coefficient, n	0.02	0.02
Upstream gate constant, c_{in}	8.3	8.3
Downstream gate constant, c_{out}	8.3	8.3

Table 1. Physical data of pool 9 and 10

3.1 Preissmann Scheme

Finite difference methods have been extensively used for simulation of complex dynamical systems, see e.g. (Chaudhry, 1993). In these methods the time, t and spatial variable, x are discretised into a grid on which the dynamical model is solved and partial derivatives are approximated in an explicit or implicit way. The approximations are based on Taylor series expansions and are called explicit if the expansion is expressed in variables available at the current time instant, it is called implicit if it involves future time instants. In the Preissmann scheme the function, $f(x, t)$ and its partial derivatives are approximated as follows ($f = A$ or Q):

$$f = \frac{1}{2}\alpha(f_{i+1}^{k+1} + f_i^{k+1}) + \frac{1}{2}(1-\alpha)(f_{i+1}^k + f_i^k)$$

$$\frac{\partial f}{\partial t} = \frac{(f_i^{k+1} + f_{i+1}^{k+1}) - (f_i^k + f_{i+1}^k)}{2\Delta t}$$

$$\frac{\partial f}{\partial x} = \frac{\alpha(f_{i+1}^{k+1} - f_i^{k+1})}{\Delta x} + \frac{(1-\alpha)(f_{i+1}^k - f_i^k)}{\Delta x}$$

Subscript i is the i^{th} spatial grid point and superscript k is the k^{th} time grid point, and Δx and Δt are the grid intervals along the x -axis and t -axis. An advantage of the Preissmann scheme is that we can have variable spatial grid. The parameter α is a weighting coefficient; the scheme is totally explicit if $\alpha = 0$. The commonly used values are $0.6 \leq \alpha \leq 0.7$ (see e.g. (Chaudhry, 1993)), and in this paper we have used $\alpha = 0.6$. The boundary condition, i.e. the equations describing the end conditions of the pool, is included directly in the system of equations that needs to be solved. The boundary condition is expressed in the following equations

$$Q_{i=1}^{k+1} - Q_a^{k+1} = 0$$

$$h_{out}^{k+1} = y_{i=np}^{k+1} - p_{max} + p_{out}^{k+1}$$

$$Q_{i=np}^{k+1} = 0 \quad \text{if } h_{out}^{k+1} < 0$$

$$Q_{i=np}^{k+1} = c(h_{out}^{k+1})^{3/2} \quad \text{otherwise}$$

where $Q_a^{k+1} = c_{in}(h_{in}^{k+1})^{3/2}$ is the discretised inflow function, where h_{in}^{k+1} and h_{out}^{k+1} are the discretised head over upstream and downstream gate, and p_{out}^{k+1} is the discretisation of the downstream gate opening. The subscript np refers to the last spatial grid point, i.e. the downstream end of the pool. Applying the approximations to the St. Venant equations, together with the boundary equations, a set of nonlinear algebraic equations is obtained. These algebraic equations can be solved using iterative search techniques, and the Newton-Raphson method is used in this paper.

4. ACCURACY OF THE ST. VENANT EQUATIONS

In this section, the St. Venant equations are compared against real data to see if they can adequately capture the dynamics of the irrigation channel. For pool 9 two data sets are available. Data set 1 is collected under low flow condition, where the channel is operated at around 25% of its capacity, while data set 2 is collected at around 75% of channel capacity.

4.1 Pool 9

Data set 1 is plotted in Figure 2 (data set 2 is not shown). The sampling interval is one minute and the gate adjustment constant is $a_9 = 23.97$. The gate constants and

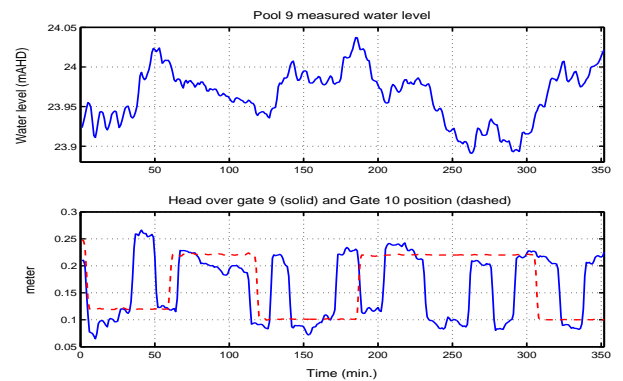


Fig. 2. Pool 9 data set 1: water level, y_{10} (top), and Head over gate 9, h_9 and gate 10 position, p_{10} (bottom)

Manning coefficient are uncertain, and these parameters $\theta = [c_{in}, c_{out}, n]$ are also estimated using the observed data. The estimation method used is a prediction error method with quadratic criterion, i.e. the criterion minimized is $\frac{1}{N} \sum_{t=1}^N \varepsilon^2(t, \theta)$, where N is the number of data points, and the prediction error, $\varepsilon(t, \theta)$ is $y(t) - \hat{y}(t, \theta)$.

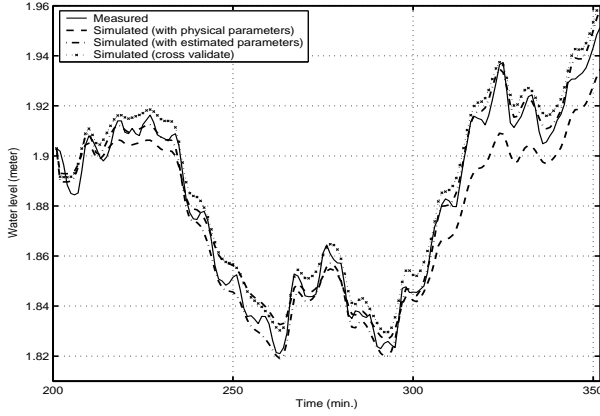


Fig. 3. Simulated and measured water levels of Pool 9 (Data set 1)

$y(t)$ and $\hat{y}(t, \theta)$ are the measured and simulated water level obtained by numerically solving the St. Venant equations. The first 200 data points in each data set were used for estimation and the rest were used for validation. The estimated gate constants and Manning coefficients are tabulated in Table 2. We next simulated the water

Estimated parameters	Measured Data 1	Measured Data 2
Manning coefficient, n	5.876×10^{-6}	2.022×10^{-2}
c_{in}	12.396	11.647
c_{out}	11.881	10.403

Table 2. Estimated parameters of pool 9

level using the St. Venant equations and compared it to the measured one. As the first 200 data points are used for estimation purposes, the comparison is based on the validation set only. The initial values of the intermediate water levels within the pool are the solution of the St. Venant equations in steady state with the last spatial grid point equalling the measured water level. The simulation is run from the beginning of the validation set where the first point of the measured water level and all the measured heads over upstream gate and measured downstream gate positions are used.

In addition to the standard validation, we also cross-validated by simulating data set 1 using the parameters estimated from data set 2 and vice-versa. Figures 3 and 4 show the simulated and measured water levels for data set 1 and 2. The Mean Squared Error (MSE) between the measured and simulated water levels are tabulated in Table 3.

Estimation set	Validation set	MSE (physical)	MSE (estimated)
Data set 1	Data set 1	1.077×10^{-4}	0.202×10^{-4}
Data set 2	Data set 2	11.11×10^{-4}	3.375×10^{-4}
Data set 1	Data set 2	-	4.690×10^{-4}
Data set 2	Data set 1	-	0.481×10^{-4}

Table 3. Mean squared errors for Pool 9

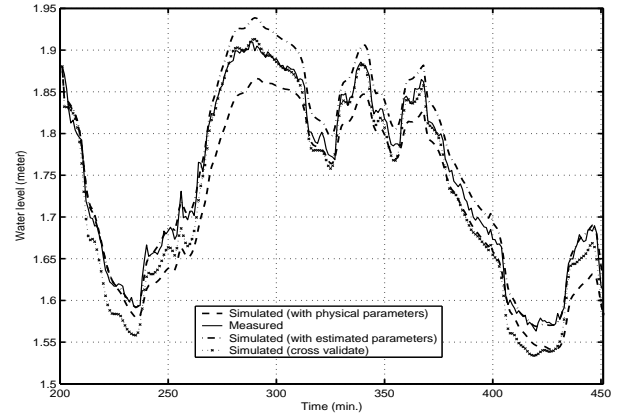


Fig. 4. Simulated and measured water levels of Pool 9 (Data set 2)

4.2 Pool 10

For pool 10, we only considered data collected under high flow condition. The sampling interval is one minute. The estimated Manning coefficient is 1.848×10^{-2} , and the estimated upstream and downstream gate constants are 11.078 and 12.382. The simulated and measured water levels are plotted in Figure 5. The MSE are 16.62×10^{-4} and 3.996×10^{-4} with physical and estimated parameters respectively.

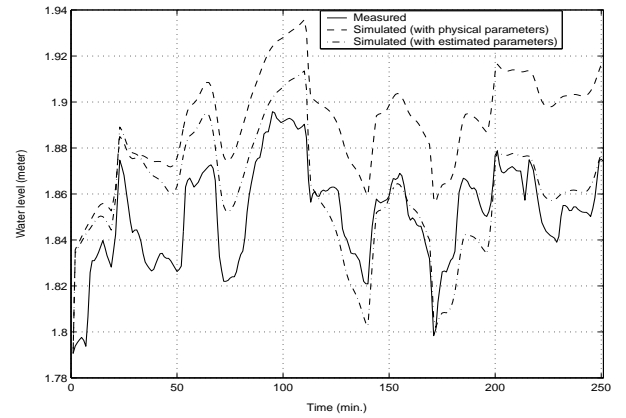


Fig. 5. Simulated and measured water levels of Pool 10

4.3 Discussion

There is good agreement between the Manning coefficient obtained from physical knowledge and the estimated ones, except the estimation using data set 1 for pool 9, where the estimated Manning coefficient is very small. Further investigations have shown that the simulated water level is insensitive to the value of the Manning coefficient. The gate constants estimated using measured data are similar to each other, but they are quite different from those computed based on physical data.

As expected, simulations using the St. Venant equations with estimated parameters give smaller MSE and the simulated water levels tracks the measured ones closer than those with physical parameters. As expected, simulations using data under low flow condition (data set 1) give smaller MSE than those under high flow condition. This is due to that larger variations in water levels are expected in the high flow condition than in the low flow condition.

In pool 9, the St. Venant equations with physical parameters are able to capture the main trends and the waves in the water level but with an offset error. The largest offset is around 3cm and 6cm for data set 1 and 2. As expected the performance is better with estimated parameters, where the models are able to accurately predict the water level with virtually no offset for data set 1, and with a small error of less than 4cm over small time periods for data set 2. Pool 10 is much longer than pool 9 and as expected the models are not as accurate as for pool 9 (larger MSE), and the largest offset is around 6cm with physical parameters. The offset is smaller with estimated parameters, around 4cm . Note that the models only have access to the initial water level, hence they are able to predict the water level ahead of time for at least $2\frac{1}{2}$ hours. The offsets can be easily corrected by integral action in a feedback controller. Therefore, apart from the offset, the St. Venant equations based purely on the physical data of the channel seem to be able to capture the relevant dynamics, at least for control purposes.

5. COMPARISON WITH SYSTEM IDENTIFICATION MODELS

In this section the system identification models and the St. Venant equations are compared. From previous works (Weyer, 2001) and (Ooi and Weyer, 2001), it is known that a first order nonlinear model is able to capture the main trends in the water level well and a third order nonlinear model is able to give very accurate predictions of the water level. The predictors associated with the first and third order models for pool i are

$$\begin{aligned} \hat{y}_{i+1}(t+1, \theta) = & \hat{y}_{i+1}(t, \theta) + c_{i,1}h_i^{3/2}(t-\tau) \\ & - c_{i+1,1}(\hat{y}_{i+1}(t, \theta) + \bar{p}_{i+1}(t) - a_{i+1})^{3/2} \end{aligned} \quad (2)$$

where $\theta = [c_{i,1}, c_{i+1,1}]$, and

$$\begin{aligned} \hat{y}_{i+1}(t+1, \theta) = & c_{i,1}h_i^{3/2}(t-\tau) + c_{i,2}h_i^{3/2}(t-\tau-1) \\ & + c_{i,3}h_i^{3/2}(t-\tau-2) + \hat{y}_{i+1}(t, \theta) \\ & + c_{i+1,1}(\hat{y}_{i+1}(t, \theta) + \bar{p}_{i+1}(t) - a_{i+1})^{3/2} \\ & + c_{i+1,2}(\hat{y}_{i+1}(t-1, \theta) + \bar{p}_{i+1}(t-1) - a_{i+1})^{3/2} \\ & + c_{i+1,3}(\hat{y}_{i+1}(t-2, \theta) + \bar{p}_{i+1}(t-2) - a_{i+1})^{3/2} \\ & + \alpha_1(\hat{y}_{i+1}(t, \theta) - 2\hat{y}_{i+1}(t-1, \theta) + \hat{y}_{i+1}(t-2, \theta)) \end{aligned}$$

$$+ \alpha_2(\hat{y}_{i+1}(t, \theta) - \hat{y}_{i+1}(t-1, \theta)) \quad (3)$$

where $\theta = [c_{i,1}, c_{i,2}, c_{i,3}, c_{i+1,1}, c_{i+1,2}, c_{i+1,3}, \alpha_1, \alpha_2]$ and τ is the time delay, and the sampling interval is one minute.

5.1 Pool 9

The unknown parameters were obtained using system identification techniques (see (Weyer, 2000) and (Weyer, 2001)) using data set 1 (see Figure 2) and 2. The first 200 and 240 data points of data set 1 and 2 respectively were used for estimation, and the rest were used for validation. The water level of the validation set is simulated using the St. Venant equations and predicted using the discrete time first and third order nonlinear models. The results are shown in Figure 6 for data set 1, and similar result are obtained for data set 2 (plot not shown). The predictor is a simulation model since it uses the predicted water level at time t to predict the level at time $t+1$, hence the comparison is fair. The mean squared errors between the measured water level and the St. Venant equations (MSE St.V), and the identification model (MSE SI) are given in Table 4. The MSE St.Vs are different from Table 3 since the simulations started at a different time instant.

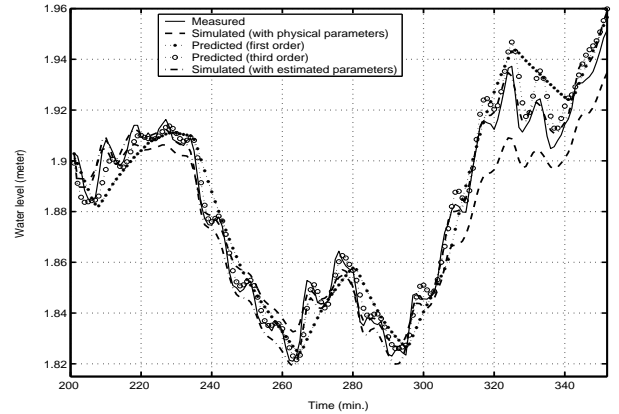


Fig. 6. Data set 1: Simulated, predicted and measured water level of pool 9

MSE St.V (physical)	MSE St.V (estimated)	MSE SI (first order)	MSE SI (third order)
1.077×10^{-4}	0.202×10^{-4}	1.107×10^{-4}	0.362×10^{-4}
10.15×10^{-4}	3.946×10^{-4}	11.652×10^{-4}	7.781×10^{-4}

Table 4. Pool 9 MSE of data set 1 (second row) and 2 (third row)

5.2 Pool 10

The same procedure is repeated for pool 10. The results are shown in Figure 7. The MSEs are given in Table 5.

MSE St.V (physical)	MSE St.V (estimated)	MSE SI (first order)	MSE SI (third order)
11.00×10^{-4}	1.96×10^{-4}	4.44×10^{-4}	1.43×10^{-4}

Table 5. *MSE* of pool 10

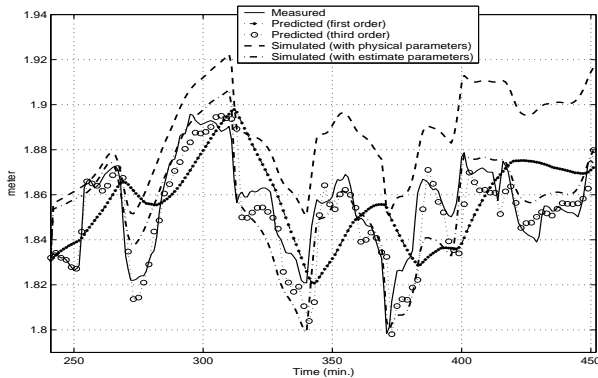


Fig. 7. Simulated, predicted and measured water level of pool 10

5.3 Discussion

In pool 9, the St. Venant equations with estimated parameters give the smallest MSE. However, the St Venant equations with physical parameters are only as accurate as the first order identification model, and the third order nonlinear identification model gives smaller MSE than the St Venant equations with physical parameters. In pool 10, the model based on the St. Venant equations with physical parameters gives largest MSE, and the third order identification model gives the smallest MSE.

Overall, there is not much difference between the St. Venant equations with estimated parameters and the third order nonlinear identification model, and both require observed data. However, the third order nonlinear model is much simpler to use for control and prediction purposes. Even a simple first order model is good enough for control design (Weyer, 2002). In the event that a new automated control scheme is to be implemented in a channel where no operational data is available, then models based on the St. Venant equations must be used. The St. Venant equations also give the water levels at the intermediate grid points, while the identification models only give the downstream water level. However, for control design purposes only the downstream water level is needed, and if there are operational data available, the system identification models are as accurate as the St. Venant equations with estimated parameters and much easier to use for control design and prediction purposes.

6. CONCLUSION

In this paper the accuracy of the St. Venant equations is examined. Water levels simulated using the St. Venant

equations with both physical and estimated parameters are compared against the measured water level. The results show that the St. Venant equations can adequately capture the dynamics of the real channels. However, the third order nonlinear identification models are as accurate as the St. Venant equations with estimated parameters but much simpler to use. Therefore, due to the complexity of the St. Venant equations, simple first and third order nonlinear models obtained using identification methods are preferred for control design and prediction purposes.

Patent: A patent has been applied for to cover the developments that are described in this paper.

Acknowledgement: This research is part of a collaborative research project between the Department of Electrical and Electronic Engineering and Rubicon Systems on modelling and control of irrigation channels. The authors would like to thank Matthew Ryan at Rubicon System in Queensland for helping carrying out the identification experiments. They would also like to thank John Fenton and Iven Mareels for many fruitful discussions on modelling and simulation of irrigation channels. This work was supported by Rubicon System Pty Ltd under the auspices of an AusIndustry Grant.

7. REFERENCES

- Brutsaert, W. (1971). De Saint-Venant equations experimentally verified. *Journal of Hyd. Div. ASCE* **97**, 1387–1401.
- Chaudhry, M. Hanif (1993). *Open-Channel Flow*. Prentice Hall.
- Fenton, J. D. (2001). *421-423: River Hydraulics (lecture note)*. The University of Melbourne.
- Malaterre, P.-O. and J.-P Baume (1998). Modeling and regulation of irrigation canals: existing applications and ongoing researches. *IEEE International Conference on Systems, Man and Cybernetics, San Diego, California* pp. 3850–3855.
- Ooi, Su Ki and E. Weyer (2001). Closed loop identification of an irrigation channel. *Proceedings of the 40th IEEE CDC, Orlando, USA* pp. 4338–4343.
- URL (2000). <http://www.lmnoeng.com/manningn.htm>. LMNO Engineering, Research, and Software, Ltd., Athens, Ohio, USA.
- Weyer, E. (2000). Analysis of September data from the Houghton Main Channel. Internal report. Department of Electrical and Electronic Engineering, University of Melbourne.
- Weyer, E. (2001). System identification of an open water channel. *Control Engineering Practise* **Vol. 9**, pp. 1289–1299.
- Weyer, E. (2002). Decentralised PI controller of an open water channel. *Proceedings of the 15th IFAC World Congress, Barcelona, Spain*.